Journal of Affective Disorders 289 (2021) 7–15

Contents lists available at ScienceDirect

Journal of Affective Disorders

journal homepage: www.elsevier.com/locate/jad

Research paper

Abnormal transitions of dynamic functional connectivity states in bipolar disorder: A whole-brain resting-state fMRI study

Mengjiao Du [a,b,c], Li Zhang [a,b,c], Linling Li [a,b,c], Erni Ji [e], Xue Han [f], Gan Huang [a,b,c], Zhen Liang [a,b,c], Li Shi [a,b,c], Haichen Yang [e,*], Zhiguo Zhang [a,b,c,d,*]

[a] School of Biomedical Engineering, Health Science Center, Shenzhen University, Shenzhen 518060, China
[b] Guangdong Provincial Key Laboratory of Biomedical Measurements and Ultrasound Imaging, Shenzhen 518060, China
[c] Marshall Laboratory of Biomedical Engineering, Shenzhen 518060, China
[d] Peng Cheng Laboratory, Shenzhen 518055, China
[e] Department for Bipolar Disorders, Shenzhen Mental Health Centre, Shenzhen Key Lab for Psychological Healthcare, Shenzhen 518020, China
[f] Department of Mental Health, Shenzhen Nanshan Center for Chronic Disease Control, Shenzhen 518060, China

ARTICLE INFO

Keywords:
Dynamic functional connectivity
bipolar disorder
functional magnetic resonance imaging
resting-state networks
zero-inflated Poisson regression

ABSTRACT

Background: Dynamic functional connectivity (dFC) based on resting-state fMRI has attracted interest in the field of bipolar disorder (BD), because dFC can better capture the evolving processes of emotion and cognition, which are typically impaired in BD. However, previous dFC studies of BD have typically focused on specific seed brain regions or specific functional brain networks, and they have ignored global dynamic information interaction in the whole brain. This study is aimed to reveal aberrant and interpretable whole-brain dFC patterns of BD.
Methods: The resting-state fMRI data collected from 35 euthymic BD patients and 30 healthy people. We developed a new dFC inference pipeline, including the sliding-window method, k-means clustering, a new permutation with zero-inflated Poisson regression method, and a similarity analysis for interpretable states, to examine the different patterns of dFC states between BD patients and healthy participants.
Results: BD patients had significantly more frequent transitions between two specific dFC states, which were respectively close to high-level cognitive networks and low-level sensory networks, than healthy controls ($p < 0.05$, FDR).
Limitations: The size of samples and other BD types need to be expanded to validate the results of this study. Possible confounding effect of medication.
Conclusions: This study detected aberrant dFC pattern of BD, which indicated the increased lability of the processes of cognition and emotion in BD, and this finding could improve our understanding of the neuropathological mechanism of BD.

1. Introduction

Bipolar disorder (BD) is a chronic and fluctuating mental disorder characterized by nonspecific symptoms, mood lability or depressive episodes. BD affects more than 1% of the global population and has a high incidence of morbidity and self-harm (Vieta et al., 2018). BD-related abnormalities in both neuroanatomical and functional organizations have been documented in previous studies (DelBello et al., 2004; Hajek et al., 2005; Malhi et al., 2005; Monks et al., 2004). BD does not only affect the functional activities in local brain regions, but also alters the functional interaction between multiple brain regions (Blumberg et al., 2003; Townsend and Altshuler, 2012; Vargas et al., 2013; Yurgelun-Todd et al., 2000). A growing number of researches show that exploring the functional brain connectivity in BD can provide insights into the neurological and pathological mechanisms of this disease.

Functional connectivity (FC) based on resting-state functional magnetic resonance imaging (fMRI) has been widely used to study mental disorders, such as BD, autism spectrum disorder, Parkinson's disease and schizophrenia (Fiorenzato et al., 2019; Fu et al., 2018; Fu et al., 2019b; Syan et al., 2018). FC is commonly inferred as the statistical interdependence between fMRI blood oxygen level dependent (BOLD) signals of

* Corresponding authors
E-mail addresses: robin518020@163.com (H. Yang), zgzhang@szu.edu.cn (Z. Zhang).

https://doi.org/10.1016/j.jad.2021.04.005
Received 26 December 2020; Received in revised form 2 April 2021; Accepted 6 April 2021
Available online 20 April 2021

two brain regions (Biswal et al., 1995; Fox and Greicius, 2010; Greicius, 2008). However, FC is conventionally estimated from the whole fMRI scan and the resultant static FC (sFC) ignores the spontaneous fluctuation of the information interaction of the brain (Calhoun et al., 2014; Hutchison et al., 2013; Preti et al., 2017). Therefore, dynamic functional connectivity (dFC) has attracted more attention as an effective tool to reveal variable and evolving functional interconnections of the brain. Many studies have shown that dFC can provide extra and meaningful information about the aberrant neural activities and underlying mechanisms of mental disorders than sFC. In the BD research field, Fateh *et al.* found that abnormal dFC was identified in the right amygdala of BD (Fateh et al., 2020), and Nguyen *et al.* reported that the dFC between the medial prefrontal cortex (mPFC) and posterior cingulate cortex (PCC) was altered in BD (Nguyen et al., 2017). BD-related dFC abnormalities did not only occur between local brain regions, but also existed between specific functional networks, which consist of a set of functionally correlated regions. Specifically, Long *et al.* reported an increase in temporal variability of dFC between the thalamus and the sensorimotor network (Long et al., 2020). Wang *et al.* found that a decreased variability of dFC between posterior default mode network (DMN) and right central executive network (CEN) in BD (Wang et al., 2020a). However, most of these dFC studies concerning BD patients were based on pre-selected seed regions or between specific brain networks, but these may entail a risk of overlooking meaningful dFC features whose nodes are not included in these pre-selected regions or networks. Recently, a whole-brain study on dFC abnormality of BD patients is still lacking. It is important to perform a whole-brain dFC analysis on BD patients, because BD-related brain abnormalities are not limited to several specific regions but are spread throughout the whole brain (Sha et al., 2019; Wang et al., 2020b; Wang et al., 2017). Particularly, the whole-brain dFC can define a set of recurring "states", which exhibit consistent patterns of spontaneous brain activities and functional connections. Many studies have linked aberrant features of whole-brain dFC states to mental disorders (Damaraju et al., 2014; Fiorenzato et al., 2019; Fu et al., 2019a; Rabany et al., 2019). For example, Fiorenzato *et al.* found that abnormal dwell time of states and number of transitions between dFC states are linked to the presence of dementia in Parkinson's disease (Fiorenzato et al., 2019). Therefore, exploring the whole-brain dFC state abnormalities of BD patients may lead to new findings in brain pathology of BD.

In the present study, we aimed to investigate the differences of whole-brain dFC states between healthy people and BD patients based on the hypothesis that the dFC states are altered in BD patients and these abnormalities in dFC states are associated with BD symptoms. To this end, we recorded resting-state fMRI data of 35 euthymic BD patients and 30 matched healthy controls. To infer distinguishable and interpretable dFC state patterns, a new dFC inference pipeline was proposed, which included the following four steps. First, we parceled the whole brain into a group of regions of interest (ROI), and then used the sliding window approach to calculate dFC and used k-means clustering to identify a small number of distinct dFC states. Second, the temporal properties of dFC states, which included the number of transitions, mean dwell time and occurrence frequency, were extracted. Third, because the temporal features of dFC states typically had a large number of zeros, which violates the assumption of conventional statistical tests, we proposed a new permutation with zero-inflated Poisson regression (PERM-ZIP) method to assess the statistical difference of dFC features between two groups. Lastly, we provided an interpretation about the identified aberrant dFC pattern according to their similarity with resting-state networks from sFC. We found that BD patients had significantly frequent transitions between two specific dFC states, which were respectively close to high-level and low-level functional networks.

2. Materials and Methods

2.1. Participants

The participants in this study comprised 35 euthymic and medicated BD type I patients (13 males, 22 females, age: 31.49±8.17 years) and 30 healthy controls (HC: 15 males, 15 females, age: 28.87±7.25 years). All BD patients were recruited from outpatient and inpatient departments at Shenzhen Mental Health Centre, and HC were recruited by advertisement. The procedures of this experiment were approved by the Human Research Ethics Committee of Shenzhen Mental Health Center, and all participants in this experiment signed an informed consent form.

The diagnostic assessment of BD was made according to the criteria of Structured Clinical Interview for DSM-IV (SCID) (Lobbestael et al., 2011), and the patients met the DSM-IV criteria for bipolar I disorder. During the experiment, the BD patients took lithium and valproate, two widely used mood stabilizer, but there was no change in psychotropic drugs or emotional state within 3 months before or during the experiment. All the patients were assessed using the Young Mania Rating Scale (YMARS) (Young et al., 1978) and Hamilton Depression Scale (HAMD) (Hamilton, 1967) before the scanning. BD patients included in this study met the following inclusion criteria: (1) all patients had ability to give voluntary informed consent; (2) the scores of YMARS and HAMD were both less than 6; (3) satisfying the criteria for undergoing MRI scanning; (4) no current depressive, manic or hypomanic episode according to SCID; (5) no history of hospitalization within 6 months. In addition, 30 HC in this work passed the following inclusion criteria: (1) no organic brain disease; (2) no history of head trauma leading to loss of consciousness for more than 10 minutes; (3) no first-degree family history of illness, which including major psychiatric illness, dementia, or mental retardation; (4) no history of alcohol or substance dependence within 12 months prior to assessment; (5) no history of psychosis or neuropathy. The non-patient version of SCID was also used to guarantee that HCs had no history of psychosis or neuropathy illness (First and Gibbon, 2004).

2.2. Data acquisition and preprocessing

The imaging data were performed on a Siemens 3T Trio scanner with a 12-channel head coil. Resting-state fMRI data were acquired using a standard gradient-echo EPI sequence with 31 oblique slices, time of repetition (TR) = 2000 ms, time of echo (TE) = 30 ms, field of view (FOV)= 240 × 240 mm^2, flip angle = 90°, size of matrix = 64 × 64, voxel size = 3 × 3 × 5 mm^3, total volume = 246. During the whole scan, all participants were requested to keep their eyes open and stay awake.

Data preprocessing procedure were carried out by using the DPABI (http://rfmri.org/dpabi/) (Yan et al., 2016) and SPM8 (https://www.fil.ion.ucl.ac.uk/spm/) toolboxes in MATLAB-R2018b (Mathworks, Sherborn, MA, US). For each subject, the first 5 volumes of resting-state fMRI data were removed, leaving 241 volumes. The middle slice was used as the reference slice for slice timing correction. Then, fMRI data were realigned to correct the head motion and obtained the 6 rigid body motion parameters. T1 images were co-registered to functional images and segmented into grey matter (GM), white matter (WM) and cerebrospinal fluid (CSF). In order to decrease the effects of head motion, the Friston 24-parameter model (6 head motion parameters, 6 head motion parameters one time point before, and the 12 corresponding squared items (Friston et al., 1996)) was used to regress out the head motion parameters. Time points with the head motion parameters larger than 0.2 were scrubbed, and they were modeled as a separate covariable for regression to decrease their influence on the continuity of time. Moreover, the WM and CFS were regressed out as the covariates, and the segmented WM and CSF images with a threshold $p > 0.99$ were used to define WM and CSF masks for each participant. The functional images were then normalized into standard Montreal Neurological Institute (MNI) space, resampled to a 3 × 3 × 3 mm^3 voxel, and smoothed with a 6 mm FWHM Gaussian kernel. Finally, a bandpass filter with a frequency

window of 0.01-0.1 Hz was used to improve the signal-to-noise ratio of signals.

2.3. Brain parcellation

We used the Dosenbach atlas to defined 160 ROIs in 6 different intrinsic connectivity networks (ICNs) (Dosenbach et al., 2010). In addition, four ROIs from bilateral amygdala and parahippocampal gyrus were added as an additional network. Therefore, a total of 7 ICNs were defined in the whole brain, and they were: cerebellum network (CER), cingulo-opercular network (CON), default mode network (DMN), fronto-parietal network (FPN), occipital network (OCC), sensorimotor network (SMN), and addition network (ADD). Then, according to the standard MNI spatial coordinates of the 164 ROIs, the radius with 8 mm was used to average the BOLD response of all voxels in the sphere, and the BOLD time courses of each ROI were extracted.

2.4. dFC estimation

The sliding window method was used to split BOLD time courses into several short segments and to calculate the whole-brain FC matrix of each segment. A tapered window with a length of 30 TR and a step of 1 TR was used to split the data, and it was obtained by convolving a rectangle window with a Gaussian window ($\sigma = 3$ TR). In each window (or say, at each time point), we calculated the Pearson's correlation coefficients between BOLD time courses of each pair of ROIs. The correlation coefficients were then transformed to z-scores by using Fisher-Z transformation. The resultant dFC matrix is the Fisher-Z-transformed correlation coefficient matrices of all time points, and it has a dimensionality of $164 \times 164 \times 211$, where 164 was the number of ROIs and 211 was the number of time points.

After the estimation of dFC, k-means clustering was applied to identify a set of dFC states, which are recurring dFC patterns. In clustering analysis, we estimated the similarity between two dFC matrices by using the L1 distance (Manhattan distance), as it is an effective similarity measure for high-dimensional data (Aggarwal et al., 2001). In order to determine the optimal number of clusters, the elbow method was used. Specifically, the upper triangle of all participants' dFC matrices were first extracted, because of the symmetry of the matrices. Then, the k-means clustering was performed in two steps. In the first step, a subset of windows that was composed of the windows with local maxima in FC variance was used as the exemplars of all participants to reduce the redundancy between windows and the computational demands. After that, the initial points of the cluster were randomly selected, which was repeated 100 times, and the result with the centroid position of the cluster was retained. In the second step, the k-means clustering was carried out on the exemplars of all participants. The centroids of the first step clustering were set as the initial points, and the number of iterations for k-means was set to 1000. Finally, all dFC matrices of all participants were clustered into 4 states according to the elbow method.

Next, a number of temporal features of these dFC states, including the number of transitions, mean dwell time, and occurrence frequency, were calculated for each participant. The number of transitions between each pair of dFC states was calculated as the number of transitions from a specific state to another state, and its value represents the lability of dFC over time. The mean dwell time and the occurrence frequency were respectively calculated as the number of continuous time point belonging to one dFC state and the percentage of one dFC state among all the time points.

2.5. Statistical analysis (PERM-ZIP)

The demographics (age and education) of BD and HC were compared using two-sample t-test. Gender difference was evaluated by the Pearson Chi-square test. The temporal features (the number of transitions, mean dwell time, and occurrence frequency) extracted from dFC states were count data containing a high proportion of zeros (i.e., zero-inflated). So, the commonly used two-sample t-test or the Wilcoxon rank-sum test are not suitable for the comparison of these dFC state features. To address this problem, we developed a new statistical comparison method, named permutation with zero-inflated Poisson regression (PERM-ZIP), which can deal with zero-inflation in count data (Chen et al., 2019; Farhadi Hassankiadeh et al., 2018; Hofmans, 2017; Lukusa and Phoa, 2020; Pew et al., 2020; Yusuf et al., 2017).

The proposed PERM-ZIP method was based on the zero-inflated Poisson regression (ZIP) model in statistics. The ZIP is a hybrid model, which consists of two models to handle a binomial process and a count process (Lambert, 1992; Yang, 2014). The probability distribution of ZIP model is as follows:

$$\mathrm{P}(Y=y_i)=\begin{cases} p_i+(1-p_i)\exp^{-\lambda}, \ for\ y_i=0, \\ (1-p_i)\lambda^{y_i}\exp^{-\lambda}/y_i!, \ for\ y_i>0. \end{cases}$$

In this model, p_i is coefficient of zero-inflated and it represents the probability of observed 0, while $1-p_i$ is the probability of observed Poisson(λ) random variable. If $0 < p_i < 1$, there is zero-inflated in data. The ZIP model reduces to the Poisson model when p_i vanishes, and the parameter λ is the mean and variance of the Poisson distribution. If the random variable Y obeys the distribution of ZIP, then its expectation and variance can be estimated as follow:

$$\mathrm{E}(Y)=(1-p_i)\lambda$$

$$\mathrm{Var}(Y)=\mathrm{E}(Y)(1+\lambda-\mathrm{E}(Y))$$

A logistic regression model is usually used for the binomial process, and a logarithmic linear model is usually used for the regression of the count process. Then, the ZIP model produced a set of parameters to model the data under study, and these parameters include intercept of the logistic regression model, coefficient of zero-inflated p_i, expectation $\mathrm{E}(Y)$ and variance $\mathrm{Var}(Y)$.

Thus, for each type of dFC feature of either BD or HC, we can use the ZIP model to fit the data and result in a number of ZIP parameters. Subsequently, we used permutation to examine whether the group difference of any ZIP model parameter between BD and HC had statistical significance. More precisely, we randomly assigned all participants into two groups (one had 35 participants and the other had 30) and such a random process was repeated 1000 times. In each permutation, we estimated the ZIP parameters for both permutation groups and calculated the differences of ZIP parameters between two permutation groups. Then, a probability density distribution of the group difference of one ZIP parameter was generated after 1000 permutations. The significance level of the actual difference of a ZIP parameter was determined by locating the actual value in the corresponding probability density contribution generated by permutation. The proposed permutation with ZIP (PERM-ZIP) method was applied for each dFC feature (the number of transitions, mean dwell time and occurrence frequency).

2.6. Similarity analysis for interpretation of dFC states

The dFC states were identified in a data-driven manner by using unsupervised clustering based on dFC matrices of all subjects (including both patients and controls). As a result, the physiological meanings of these states were not straightforward. In order to better interpret the identified aberrant dFC states, we compared each dFC state with the well-established ICNs as revealed by the sFC, which has been well studied and have relatively clear meanings and interpretations. This comparison was achieved by calculating the similarity (in terms of L1 distance) between the dFC state and sFC. If a dFC state and sFC had a smaller L1 distance, the higher similarity they had. We used ANOVA and post-hoc test to detect whether there were significant differences in the similarity between each of the four dFC states and sFC. We further checked the similarity between dFC states and sFC for each pair of ICN.

Because there were 7 ICNs, we had 7 within-network pairs and 21 inter-network pairs. Similarly, ANOVA and post-hoc test was used to examine whether there were significant differences in the similarity between each dFC state and sFC for each network-pair. The false discovery rate (FDR) (Benjamini and Hochberg, 1995) was applied to address the problem of multiple comparisons.

3. Results

3.1. Demographic characteristics

The demographic characteristics of all participants in this analysis are shown in Table 1. There were no significant differences in gender, age, and education between 35 BD patients and 30 HC.

3.2. dFC states

Fig. 1A shows the sFC pattern estimated from the whole scan and averaged from all participants. Through the sliding window and group-level k-means clustering analysis, we determined four states of dFC, of which the centroids were displayed in Fig. 1B. The proportions of states 1-4 in all time points of all participants are 9%, 19%, 26%, and 46%, respectively.

3.3. Comparisons of dFC state features between BD and HC

We used PERM-ZIP to analyze the group differences of dFC state features (the number of transitions, the mean dwell time, and the occurrence frequency) between BD and HC. We found expectation, the ZIP parameter representing the weighted mean of the variable, of the number of transitions between state 3 and state 4 had significant differences between two groups. The greater expectation of the BD group means the transitions between state 3 and state 4 in BD were significantly more frequent than those in HC. Results displayed in Fig. 2A show that the number of transitions from state 3 to state 4 and the number of transitions from state 4 to state 3 in BD (state 3 to state 4: 1.49±1.07; state 4 to state 3: 1.51±1.15) were significantly higher than those in HC (state 3 to state 4: 0.83±0.99; state 4 to state 3: 0.83±0.95) ($p < 0.05$, FDR corr.). For the other two features (the mean dwell time and the occurrence frequency), there were no significant differences between BD and HC, as shown in Fig. 2B and C. The state transitions of two examples were shown in Fig. 2D.

Table 1
Demographic data of the patients with bipolar disorder and healthy controls in this experiment

	BD		HC		P value
No. of subjects (male/female)	35 (13/22)		30 (15/15)		0.297[a]
	Mean (SD)	Min−Max	Mean (SD)	Min−Max	BD vs. HC
Age (years)	31.49 (8.17)	18−54	28.87 (7.25)	22−47	0.180[b]
Education (years)	13.40 (2.93)	8−18	14.43 (2.89)	8−18	0.159[b]
HAMD	1.11 (1.32)	0−3	–	–	–
YMRS	0.71 (0.93)	0−4	–	–	–
Duration of illness (years)	8.51 (6.46)	0.25−24	–	–	–
No. of manic episodes	2.54 (1.60)	1−6	–	–	–
No. of depressive episodes	1.60 (1.50)	0−8	–	–	–

Note: HAMD: Hamilton Depression Scale; YMRS: Young Mania Rating Scale.
[a] Pearson Chi-square test
[b] independent two-sample t-test

3.4. Characteristics of dFC states

With the aim to better interpret dFC states, we further explored the similarity between dFC states and sFC by calculating the L1 distance between them at the whole-brain level and at the network level for all subjects in both HC and BD groups. The results were displayed in Fig. 3. It can be seen from Fig. 3A that the L1 distance between state 3 and sFC is the smallest, followed by that between state 4 and sFC, suggesting that state 3 and state 4 are the most and the second most similar states to sFC at the whole-brain level. To further check the similarity between sFC and these two similar states (state 3 and state 4) at the block network level, we estimated the L1 distance between state 3 or state 4 and sFC in 28 network pairs (7 within-network pairs and 21 between-network pairs). The results were shown in Fig. 3B, which indicated that state 3 and sFC had significantly higher similarity in high-level network-pairs, such as DMN-CON, within-DMN, DMN-FPN, FPN-CON and within-FPN ($p < 0.05$, FDR), which are mainly involved in high-level cognitive functions. On the other hand, state 4 and sFC had significantly higher similarity in low-level network pairs, such as SMN-OCC, SMN-DMN, and within-SMN ($p < 0.05$, FDR), which mainly subserve low-level sensory functions. Thus, state 3 could be interpreted as a sFC-like high-level state, while state 4 could be interpreted as a sFC-like low-level state.

4. Discussion

In the present study, we investigated BD-related abnormalities in whole-brain dFC states. Our main finding is that, the number of transitions between two dFC states (state 3 and state 4, which were respectively considered as a high-level state and a low-level state), was significantly different between BD and HC. Thus, the aberrant transition between these two dFC states could be an important neuroimaging signature for the neuropathology associated with BD.

4.1. Recurring dFC states

dFC can indicate the flexibility and adaptability of the functional brain networks, so it has been widely used in the research of mental diseases in the past few years. Our findings and other research on psychiatric disorders suggest the importance of assessing the transients and fluctuations of FC. Previous studies have shown BD-related local abnormal dFC is associated with abnormal emotional and cognitive processes. However, emotion and cognitive processes are highly complex and involve the interaction of multiple brain networks, such as sensory, motor, and control networks (Perry et al., 2019; Tononi et al., 1994). Hence, only considering abnormal dFC between several local brain regions and individual networks in BD may ignore valuable information about the abnormal brain's information communication during the processes of emotion and cognition. In addition, dFC state analysis is an advanced method to explore the evolution of the whole brain network configuration. The whole-brain dFC states can capture the transient changes of all functional brain networks and can be used to further explore recurring functional brain states based on the highly variable interaction in the brain (Allen et al., 2014). So, in the present study we finally identified four recurring dFC states, which represented similar whole-brain FC configurations among multiple time points and participants. In particular, state 3 was the most similar state to sFC in network-pairs involving high-level cognitive functions, such as CON, DMN and FPN, while state 4 was the most similar state to sFC in network-pairs involving low-level sensory functions, such as OCC and SMN. More specifically, CON, DMN and FPN play an important role in high-level cognition and emotion, and they can coordinate and modulate low-level sensory and perceptual networks, such as OCC and SMN, through top-down modulation (Yuan et al., 2019). Thus, state 3 and state 4 were referred to sFC-like high-level state and sFC-like low-level state, respectively. In addition, sFC (static FC) is much more extensively used to investigate psychiatric disorders than dFC in resting-state fMRI

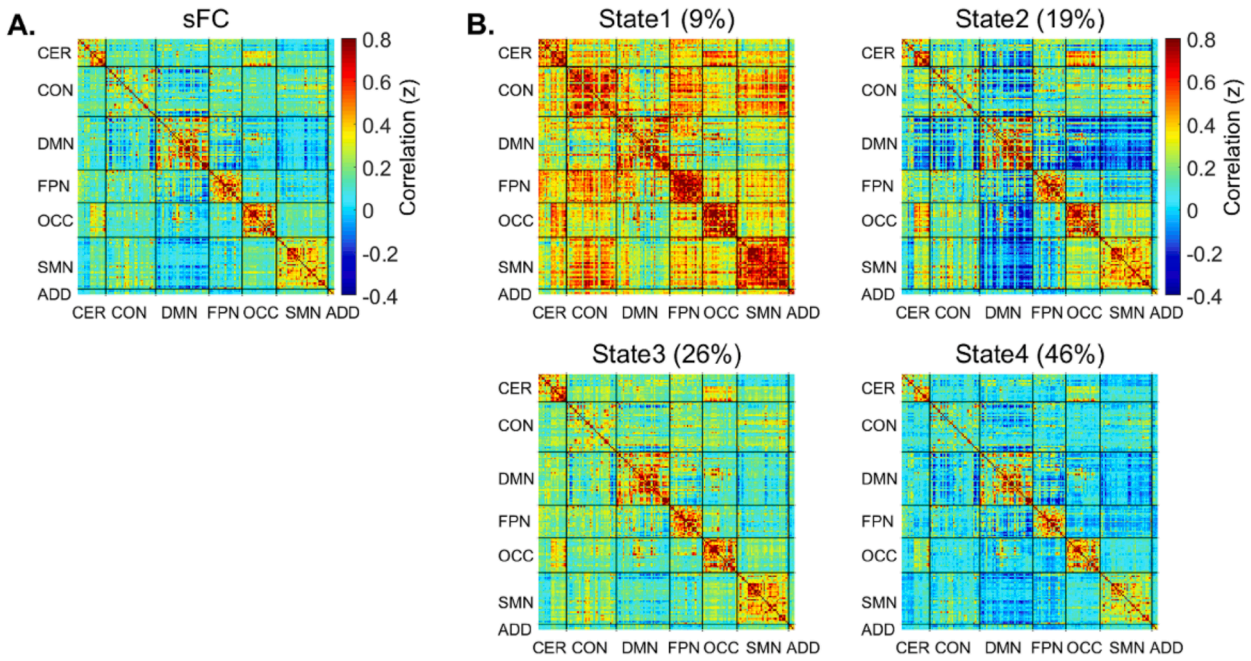

Fig. 1. A. sFC was obtained from the whole fMRI scan and averaged across all participants. B. Four dFC states were illustrated by their centroids. The numbers in parentheses were the proportions of the four dFC states in all time points of all participants.

studies. We compared the sFC between BD and HC but found no difference, which means that BD patients do not have aberrant static functional brain networks.

4.2. Aberrant transitions of dFC states in BD

Our findings revealed the aberrant transitions between two distinct sFC-like dFC states in BD patients. Normally, dFC analysis assumes that the whole-brain's functional networks vary among several dFC states, and dFC transitions describe the patterns of variations in dFC states and indicate the stability and volatility of the brain's functional networks. Abnormal patterns of dFC transitions have been related to several types of psychiatric disorders (Cao et al., 2019; Fiorenzato et al., 2019; Li et al., 2020; Liu et al., 2017). We can see from the literature that, the number of transitions between dFC states can reflect the dynamics, flexibility, and efficiency of information transmission in the brain's functional networks. Normal brain functions depend on a stable and effective transmission of information between brain functional networks and abnormal patterns of dFC transitions are often related to psychiatric disorders. These results are consistent with our findings. Compared with HC, BD patients had significantly larger number of transitions between state 3 and state 4, which can be interpreted as follows. BD is characterized by emotional dysregulation, fluctuating affections and cognitive deficits (Bonsall et al., 2015; Leibenluft, 2011; Vieta et al., 2018), so that emotion, affection, and cognition of BD patients fluctuate greatly (Renaud et al., 2012). A loss of stability in large-scale brain dynamics has be well validated in BD in recent researches. Emotional dysregulation of BD patients arises from dynamic lability in interoceptive circuit and cognitive control system (Perry et al., 2019). The abnormal temporal properties of electroencephalographic (EEG) microstates (Damborská et al., 2019) and effective connectivity based on fMRI (de Almeida et al., 2009; Radaelli et al., 2015) also support the dysregulation of emotion-related networks in BD. In addition, the emotional instability of BD patients can be attributed to the emotional and cognitive dysfunction (Bilderbeck et al., 2016; Green et al., 2007; Lima et al., 2018). Therefore, the instability of dFC states (especially the transitions between high-level and low-level sFC networks) identified in the present study may be related to emotional and cognitive disorders, including but not limited to BD.

Specifically, state 3 was characterized as an sFC-like high-level cognitive state, while state 4 was characterized as an sFC-like low-level sensory state. So, the frequency of transitions between state 3 and state 4 could represent how the brain shifts from sensory processing to cognitive functioning. Those dominant networks in state 3 (CON, DMN and FPN) are high-level cognitive networks which can coordinate other networks (such as OCC and SMN) to process external and internal information (Buckner and Carroll, 2007; Smallwood et al., 2012) and can support cognition, perception, emotion and social interactions (Menon, 2011). More precisely, CON and FPN are considered indispensable for cognitive flexibility. For example, during the performance of some complex cognitive tasks, both FPN and CON display increased activity (Dosenbach et al., 2007; Sheffield et al., 2015). FPN provides information regarding control and regulation for CON, while CON integrates sensory information to evaluate the homeostatic relevance of stimuli and affects the information processing of downstream (Dosenbach et al., 2008). DMN also participates in emotional and cognitive functions and inner-thoughts (Martino et al., 2016). FC abnormalities among FPN, DMN and CON are often related to emotional and cognitive impairment, and have been reported in BD patients (Goya-Maldonado et al., 2016; Lois et al., 2014). On the other hand, those dominant networks in state 4 (SMN and OCC) are typical sensory networks which can perceive the stimuli from external or internal environments, activate and contextualize the sensory information (Dong et al., 2019; Perry et al., 2019).

Some studies suggested that the neural modelling of emotion regulation is considered as the interaction between bottom-up emotional evaluation and top-down cognitive control (Phillips et al., 2008). Cognition provides a framework for evaluating internal and external stimuli, and the capabilities of cognition can affect the way of emotional regulation (Lima et al., 2018; Oatley and Johnson-Laird, 2014). Moreover, the way of thinking, feeling and behavior is affected by emotion, and they can be regulated in various ways. When emotion regulation is scarce, or poorly matched to situational requirements, the emotional responses may be inappropriate, insufficient or excessive(Aldao et al., 2010; Etkin et al., 2015). The whole-brain dFC patterns are widely associated with the emotion and cognition, so the low-level sensory and high-level cognition should be represented by distinct dFC patterns. The

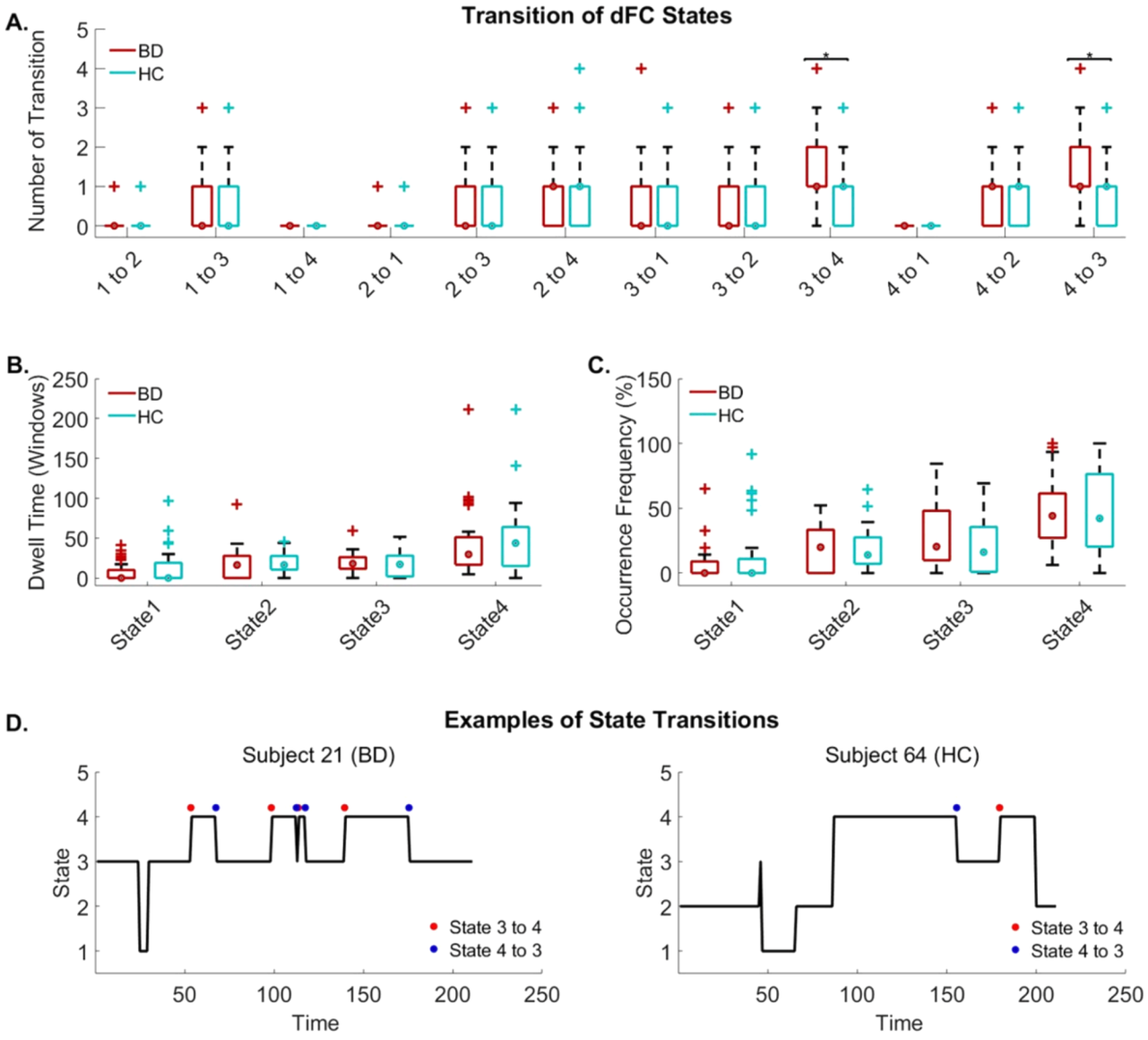

Fig. 2. Comparisons of dFC state features between BD and HC. A. The number of transitions between states. B. The mean dwell time. C. The occurrence frequency. BD is marked in red, and HC is marked in green. On each box plot, the central circle denotes the median; the edges of the box are the 25th and 75th percentiles. * $p < 0.05$, FDR. D. Examples of state transitions of two participants. A red dot represents a transition from state 3 to state 4, while a blue dot represents a transition from state 4 to state 3. There are more transitions between state 3 and state 4 in BD than HC.

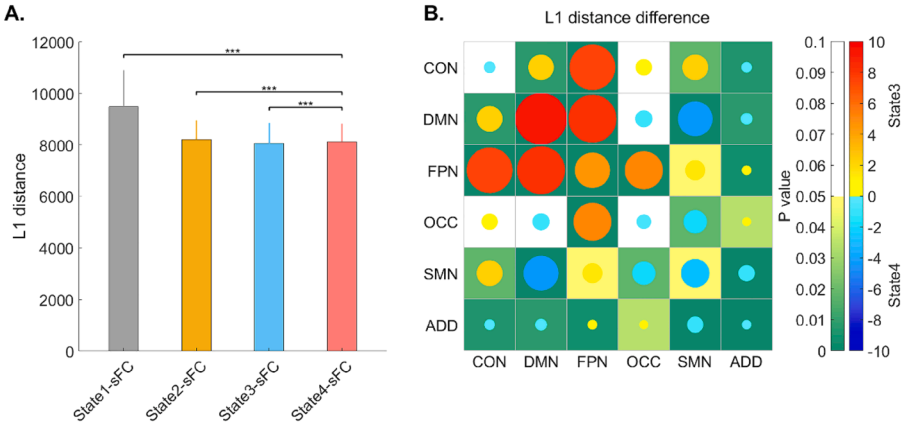

Fig. 3. A. Comparisons of similarity between dFC states and sFC, as measured by L1 distance between the whole-brain FC matrices (*** $p < 0.001$, FDR) of all subjects in both HC and BD groups. dFC state 3 and state 4 are the most and the second most similar states to sFC. B. Comparisons of similarity between dFC state 3 and state 4 in each network-pair of all subjects in both HC and BD groups. The similarity between state 3 or 4 and sFC and the extent of the similarity were respectively coded by the color and size of circles. If state 3 of one network-pair was more similar to sFC, then the corresponding circle had a color closer to red and a larger size. On the contrary, if state 4 of one network-pair was more similar to sFC, then the corresponding circle had a color closer to blue and a larger size.

number of transitions between these two states in BD was more frequent than HC, which indicated the instability of transitions between high-level networks and low-level networks in BD. It may also imply a loss of stability in the large-scale functional brain network and a less efficient transmission of information between high-level and low-level networks. So, the patients with BD cannot normally participate in top-down cognitive control and bottom-up emotional assessment, and then may have insufficient ability to regulate emotion and execute cognitive tasks. In addition, one recent EEG study showed that there were more frequent transitions between EEG microstates in BD patients, which agreed with our findings well (Vellante et al., 2020).

Taken together, the frequency of transitions between the low-level state 3 and the high-level state 4 indicates the lability of the processes of cognition and emotion in BD. Failure or insufficiency in the regulation and control related brain activities and networks may cause disorders in emotion and cognition.

4.3. Limitations and future work

There are some issues that may be worth investigating in the future. Firstly, although the abnormalities of dFC states were found in BD and were considered as the reason of affection lability in BD, it remains unclear whether these dFC abnormalities are specific to BD or not. Second, the patients recruited in the present study only included BD I type, which may limit the extension of our results to other BD subtypes. To check the common and specific patterns of dFC in different mental disorders with emotional symptoms and other subtypes of BD will be interesting. In the future work, expanding the size of samples and the including more centers or sites are important to verify or generalize the results in this study. Third, mood stabilizers and antipsychotics were prescribed for all patients, and anticonvulsants, antidepressants or anxiolytics were prescribed for a small number of patients. Different medications might interact to produce different effects, so medication could be a confounding factor of our study. Last but not least, with the rapid development of dFC analysis, more meaningful dFC features could be available so that more information about BD can be extracted from the dynamic patterns of FC, providing effective tools to reveal the neural mechanism of BD.

5. Conclusion

This study investigated the temporal properties of dFC states in BD patients. We found that the number of transitions between an sFC-like high-level cognitive state and an sFC-like low-level sensory state was significantly higher in BD. These aberrant frequency of transitions between dFC states may potentially be an important and objective neuroimaging marker for BD. These results suggest that whole-brain dFC analysis is a useful tool to reveal abnormal dynamic brain states in BD patients and the finding can improve our understanding of the neural mechanisms of BD from a new perspective.

Ethical approval

All procedures performed in this study were approved by the Human Research Ethics Committee of the Shenzhen Mental Health center, and were conducted in accordance with the 1964 Helsinki declaration and its later amendments.

Authors contribution

Mengjiao Du, Li Zhang and Zhiguo Zhang designed the study and developed the theoretical framework. Erni Ji and Xue Han contributed to data curation. Mengjiao Du analyzed the data and wrote the original draft. Li Zhang, Huang Gan, Zhen Liang and Shi Li contributed to results discussion. Zhiguo Zhang and Haichen Yang contributed to funding acquisition. Mengjiao Du, Li Zhang, Linglin Li and Zhiguo Zhang review and editing the manuscript. All authors contributed to the final version of the manuscript.

Declaration of Competing Interest

The authors declare that they have no known competing financial interests or personal relationships that could have appeared to influence the work reported in this paper.

Funding

This work was supported by the National Natural Science Foundation of China (no. 81871443, 81901831), the Sanming Project of Medicine in Shenzhen (no. SZSM201612006), the Science, Technology and Innovation Commission of Shenzhen Municipality Technology Fund (no. JCYJ20170818093322718), the Shenzhen Peacock Plan (no. KQTD2016053112051497), the Shenzhen Key Medical Discipline Construction Fund (no. SZXK043), and the Shenzhen Fund for Guangdong Provincial High-level Clinical Key Specialties (no. SZGSP013).

Acknowledgments

We thank all the participants for participating in our study.

Supplementary materials

Supplementary material associated with this article can be found, in the online version, at doi:10.1016/j.jad.2021.04.005.

References

Aggarwal, C.C., Hinneburg, A., Keim, D.A., 2001. On the surprising behavior of distance metrics in high dimensional space. International conference on database theory. Springer, pp. 420–434.
Aldao, A., Nolen-Hoeksema, S., Schweizer, S., 2010. Emotion-regulation strategies across psychopathology: A meta-analytic review. Clinical psychology review 30, 217–237.
Allen, E.A., Damaraju, E., Plis, S.M., Erhardt, E.B., Eichele, T., Calhoun, V.D., 2014. Tracking whole-brain connectivity dynamics in the resting state. Cerebral cortex 24, 663–676.
Benjamini, Y., Hochberg, Y., 1995. Controlling the false discovery rate: a practical and powerful approach to multiple testing. Journal of the Royal statistical society: series B (Methodological) 57, 289–300.
Bilderbeck, A., Reed, Z.E., McMahon, H., Atkinson, L., Price, J., Geddes, J., Goodwin, G., Harmer, C., 2016. Associations between mood instability and emotional processing in a large cohort of bipolar patients. Psychological medicine 46, 3151–3160.
Biswal, B., Zerrin Yetkin, F., Haughton, V.M., Hyde, J.S., 1995. Functional connectivity in the motor cortex of resting human brain using echo-planar MRI. Magnetic resonance in medicine 34, 537–541.
Blumberg, H.P., Leung, H.-C., Skudlarski, P., Lacadie, C.M., Fredericks, C.A., Harris, B.C., Charney, D.S., Gore, J.C., Krystal, J.H., Peterson, B.S., 2003. A functional magnetic resonance imaging study of bipolar disorder: state-and trait-related dysfunction in ventral prefrontal cortices. Archives of general psychiatry 60, 601–609.
Bonsall, M.B., Geddes, J.R., Goodwin, G.M., Holmes, E.A., 2015. Bipolar disorder dynamics: affective instabilities, relaxation oscillations and noise. Journal of the Royal Society Interface 12, 20150670.
Buckner, R.L., Carroll, D.C., 2007. Self-projection and the brain. Trends in cognitive sciences 11, 49–57.
Calhoun, V.D., Miller, R., Pearlson, G., Adalı, T., 2014. The chronnectome: time-varying connectivity networks as the next frontier in fMRI data discovery. Neuron 84, 262–274.
Cao, B., Chen, Y., Yu, R., Chen, L., Chen, P., Weng, Y., Chen, Q., Song, J., Xie, Q., Huang, R., 2019. Abnormal dynamic properties of functional connectivity in disorders of consciousness. NeuroImage: Clinical 24, 102071.
Chen, K., Huang, R., Chan, N.H., Yau, C.Y., 2019. Subgroup analysis of zero-inflated Poisson regression model with applications to insurance data. Insurance: Mathematics and Economics 86, 8–18.
Damaraju, E., Allen, E.A., Belger, A., Ford, J.M., McEwen, S., Mathalon, D., Mueller, B., Pearlson, G., Potkin, S., Preda, A., 2014. Dynamic functional connectivity analysis reveals transient states of dysconnectivity in schizophrenia. NeuroImage: Clinical 5, 298–308.
Damborská, A., Piguet, C., Aubry, J.-M., Dayer, A.G., Michel, C.M., Berchio, C., 2019. Altered EEG resting-state large-scale brain network dynamics in euthymic bipolar disorder patients. Frontiers in Psychiatry 10, 826.
de Almeida, J.R.C., Versace, A., Mechelli, A., Hassel, S., Quevedo, K., Kupfer, D.J., Phillips, M.L., 2009. Abnormal amygdala-prefrontal effective connectivity to happy faces differentiates bipolar from major depression. Biological psychiatry 66, 451–459.

DelBello, M.P., Zimmerman, M.E., Mills, N.P., Getz, G.E., Strakowski, S.M., 2004. Magnetic resonance imaging analysis of amygdala and other subcortical brain regions in adolescents with bipolar disorder. Bipolar disorders 6, 43–52.
Dong, D., Duan, M., Wang, Y., Zhang, X., Jia, X., Li, Y., Xin, F., Yao, D., Luo, C., 2019. Reconfiguration of dynamic functional connectivity in sensory and perceptual system in schizophrenia. Cerebral Cortex 29, 3577–3589.
Dosenbach, N.U., Fair, D.A., Cohen, A.L., Schlaggar, B.L., Petersen, S.E., 2008. A dual-networks architecture of top-down control. Trends in cognitive sciences 12, 99–105.
Dosenbach, N.U., Fair, D.A., Miezin, F.M., Cohen, A.L., Wenger, K.K., Dosenbach, R.A., Fox, M.D., Snyder, A.Z., Vincent, J.L., Raichle, M.E., 2007. Distinct brain networks for adaptive and stable task control in humans. Proceedings of the National Academy of Sciences 104, 11073–11078.
Dosenbach, N.U., Nardos, B., Cohen, A.L., Fair, D.A., Power, J.D., Church, J.A., Nelson, S. M., Wig, G.S., Vogel, A.C., Lessov-Schlaggar, C.N., 2010. Prediction of individual brain maturity using fMRI. Science 329, 1358–1361.
Etkin, A., Büchel, C., Gross, J.J., 2015. The neural bases of emotion regulation. Nature reviews neuroscience 16, 693–700.
Farhadi Hassankiadeh, R., Kazemnejad, A., Gholami Fesharaki, M., Kargar Jahromi, S., 2018. Efficiency of zero-inflated generalized poisson regression model on hospital length of stay using real data and simulation study. Caspian Journal of Health Research 3, 5–9.
Fateh, A.A., Cui, Q., Duan, X., Yang, Y., Chen, Y., Li, D., He, Z., Chen, H., 2020. Disrupted dynamic functional connectivity in right amygdalar subregions differentiates bipolar disorder from major depressive disorder. Psychiatry Research: Neuroimaging 304, 111149.
Fiorenzato, E., Strafella, A.P., Kim, J., Schifano, R., Weis, L., Antonini, A., Biundo, R., 2019. Dynamic functional connectivity changes associated with dementia in Parkinson's disease. Brain 142, 2860–2872.
First, M.B., Gibbon, M., 2004. The structured clinical interview for DSM-IV axis I disorders (SCID-I) and the structured clinical interview for DSM-IV axis II disorders (SCID-II). Comprehensive handbook of psychological assessment 2, 134–143.
Fox, M.D., Greicius, M., 2010. Clinical applications of resting state functional connectivity. Frontiers in systems neuroscience 4, 19.
Friston, K.J., Williams, S., Howard, R., Frackowiak, R.S., Turner, R., 1996. Movement-related effects in fMRI time-series. Magnetic resonance in medicine 35, 346–355.
Fu, Z., Caprihan, A., Chen, J., Du, Y., Adair, J.C., Sui, J., Rosenberg, G.A., Calhoun, V.D., 2019a. Altered static and dynamic functional network connectivity in Alzheimer's disease and subcortical ischemic vascular disease: shared and specific brain connectivity abnormalities. Human Brain Mapping 40, 3203–3221.
Fu, Z., Tu, Y., Di, X., Du, Y., Pearlson, G.D., Turner, J.A., Biswal, B.B., Zhang, Z., Calhoun, V.D., 2018. Characterizing dynamic amplitude of low-frequency fluctuation and its relationship with dynamic functional connectivity: an application to schizophrenia. Neuroimage 180, 619–631.
Fu, Z., Tu, Y., Di, X., Du, Y., Sui, J., Biswal, B.B., Zhang, Z., de Lacy, N., Calhoun, V.D., 2019b. Transient increased thalamic-sensory connectivity and decreased whole-brain dynamism in autism. Neuroimage 190, 191–204.
Goya-Maldonado, R., Brodmann, K., Keil, M., Trost, S., Dechent, P., Gruber, O., 2016. Differentiating unipolar and bipolar depression by alterations in large-scale brain networks. Human brain mapping 37, 808–818.
Green, M.J., Cahill, C.M., Malhi, G.S., 2007. The cognitive and neurophysiological basis of emotion dysregulation in bipolar disorder. Journal of affective disorders 103, 29–42.
Greicius, M., 2008. Resting-state functional connectivity in neuropsychiatric disorders. Current opinion in neurology 21, 424–430.
Hajek, T., Carrey, N., Alda, M., 2005. Neuroanatomical abnormalities as risk factors for bipolar disorder. Bipolar disorders 7, 393–403.
Hamilton, M., 1967. Development of a rating scale for primary depressive illness. British journal of social and clinical psychology 6, 278–296.
Hofmans, J., 2017. Modeling psychological contract violation using dual regime models: an event-based approach. Frontiers in psychology 8, 1948.
Hutchison, R.M., Womelsdorf, T., Allen, E.A., Bandettini, P.A., Calhoun, V.D., Corbetta, M., Della Penna, S., Duyn, J.H., Glover, G.H., Gonzalez-Castillo, J., 2013. Dynamic functional connectivity: promise, issues, and interpretations. Neuroimage 80, 360–378.
Lambert, D., 1992. Zero-inflated Poisson regression, with an application to defects in manufacturing. Technometrics 34, 1–14.
Leibenluft, E., 2011. Severe mood dysregulation, irritability, and the diagnostic boundaries of bipolar disorder in youths. American Journal of Psychiatry 168, 129–142.
Li, Y., Zhu, Y., Nguchu, B.A., Wang, Y., Wang, H., Qiu, B., Wang, X., 2020. Dynamic functional connectivity reveals abnormal variability and hyper-connected pattern in autism spectrum disorder. Autism Research 13, 230–243.
Lima, I.M., Peckham, A.D., Johnson, S.L., 2018. Cognitive deficits in bipolar disorders: Implications for emotion. Clinical psychology review 59, 126–136.
Liu, F., Wang, Y., Li, M., Wang, W., Li, R., Zhang, Z., Lu, G., Chen, H., 2017. Dynamic functional network connectivity in idiopathic generalized epilepsy with generalized tonic–clonic seizure. Human brain mapping 38, 957–973.
Lobbestael, J., Leurgans, M., Arntz, A., 2011. Inter-rater reliability of the Structured Clinical Interview for DSM-IV Axis I disorders (SCID I) and Axis II disorders (SCID II). Clinical psychology & psychotherapy 18, 75–79.
Lois, G., Linke, J., Wessa, M., 2014. Altered functional connectivity between emotional and cognitive resting state networks in euthymic bipolar I disorder patients. PLoS One 9, e107829.
Long, Y., Liu, Z., Chan, C.K.Y., Wu, G., Xue, Z., Pan, Y., Chen, X., Huang, X., Li, D., Pu, W., 2020. Altered Temporal Variability of Local and Large-Scale Resting-State Brain Functional Connectivity Patterns in Schizophrenia and Bipolar Disorder. Frontiers in Psychiatry 11, 422.
Lukusa, M.T., Phoa, F.K.H., 2020. A Horvitz-type estimation on incomplete traffic accident data analyzed via a zero-inflated Poisson model. Accident Analysis & Prevention 134, 105235.
Malhi, G.S., Lagopoulos, J., Sachdev, P.S., Ivanovski, B., Shnier, R., 2005. An emotional Stroop functional MRI study of euthymic bipolar disorder. Bipolar disorders 7, 58–69.
Martino, M., Magioncalda, P., Huang, Z., Conio, B., Piaggio, N., Duncan, N.W., Rocchi, G., Escelsior, A., Marozzi, V., Wolff, A., 2016. Contrasting variability patterns in the default mode and sensorimotor networks balance in bipolar depression and mania. Proceedings of the National Academy of Sciences 113, 4824–4829.
Menon, V., 2011. Large-scale brain networks and psychopathology: a unifying triple network model. Trends in cognitive sciences 15, 483–506.
Monks, P.J., Thompson, J.M., Bullmore, E.T., Suckling, J., Brammer, M.J., Williams, S.C., Simmons, A., Giles, N., Lloyd, A.J., C., Louise Harrison, 2004. A functional MRI study of working memory task in euthymic bipolar disorder: evidence for task-specific dysfunction. Bipolar disorders 6, 550–564.
Nguyen, T.T., Kovacevic, S., Dev, S.I., Lu, K., Liu, T.T., Eyler, L.T., 2017. Dynamic functional connectivity in bipolar disorder is associated with executive function and processing speed: A preliminary study. Neuropsychology 31, 73.
Oatley, K., Johnson-Laird, P.N., 2014. Cognitive approaches to emotions. Trends in cognitive sciences 18, 134–140.
Perry, A., Roberts, G., Mitchell, P.B., Breakspear, M., 2019. Connectomics of bipolar disorder: a critical review, and evidence for dynamic instabilities within interoceptive networks. Molecular psychiatry 24, 1296–1318.
Pew, T., Warr, R.L., Schultz, G.G., Heaton, M., 2020. Justification for considering zero-inflated models in crash frequency analysis. Transportation Research Interdisciplinary Perspectives 8, 100249.
Phillips, M.L., Ladouceur, C.D., Drevets, W.C., 2008. A neural model of voluntary and automatic emotion regulation: implications for understanding the pathophysiology and neurodevelopment of bipolar disorder. Molecular psychiatry 13, 833–857.
Preti, M.G., Bolton, T.A., Van De Ville, D., 2017. The dynamic functional connectome: State-of-the-art and perspectives. Neuroimage 160, 41–54.
Rabany, L., Brocke, S., Calhoun, V.D., Pittman, B., Corbera, S., Wexler, B.E., Bell, M.D., Pelphrey, K., Pearlson, G.D., Assaf, M., 2019. Dynamic functional connectivity in schizophrenia and autism spectrum disorder: Convergence, divergence and classification. NeuroImage: Clinical 24, 101966.
Radaelli, D., Papa, G.S., Vai, B., Poletti, S., Smeraldi, E., Colombo, C., Benedetti, F., 2015. Fronto-limbic disconnection in bipolar disorder. European Psychiatry 30, 82–88.
Renaud, S., Corbalan, F., Beaulieu, S., 2012. Differential diagnosis of bipolar affective disorder type II and borderline personality disorder: analysis of the affective dimension. Comprehensive psychiatry 53, 952–961.
Sha, Z., Wager, T.D., Mechelli, A., He, Y., 2019. Common dysfunction of large-scale neurocognitive networks across psychiatric disorders. Biological psychiatry 85, 379–388.
Sheffield, J.M., Repovs, G., Harms, M.P., Carter, C.S., Gold, J.M., MacDonald III, A.W., Ragland, J.D., Silverstein, S.M., Godwin, D., Barch, D.M., 2015. Fronto-parietal and cingulo-opercular network integrity and cognition in health and schizophrenia. Neuropsychologia 73, 82–93.
Smallwood, J., Brown, K., Baird, B., Schooler, J.W., 2012. Cooperation between the default mode network and the frontal–parietal network in the production of an internal train of thought. Brain research 1428, 60–70.
Syan, S.K., Smith, M., Frey, B.N., Remtulla, R., Kapczinski, F., Hall, G.B., Minuzzi, L., 2018. Resting-state functional connectivity in individuals with bipolar disorder during clinical remission: a systematic review. Journal of psychiatry & neuroscience: JPN 43, 298.
Tononi, G., Sporns, O., Edelman, G.M., 1994. A measure for brain complexity: relating functional segregation and integration in the nervous system. Proceedings of the National Academy of Sciences 91, 5033–5037.
Townsend, J., Altshuler, L.L., 2012. Emotion processing and regulation in bipolar disorder: a review. Bipolar disorders 14, 326–339.
Vargas, C., López-Jaramillo, C., Vieta, E., 2013. A systematic literature review of resting state network—functional MRI in bipolar disorder. Journal of affective disorders 150, 727–735.
Vellante, F., Ferri, F., Baroni, G., Croce, P., Migliorati, D., Pettoruso, M., De Berardis, D., Martinotti, G., Zappasodi, F., Di Giannantonio, M., 2020. Euthymic bipolar disorder patients and EEG microstates: a neural signature of their abnormal self experience? Journal of affective disorders 272, 326–334.
Vieta, E., Berk, M., Schulze, T.G., Carvalho, A.F., Suppes, T., Calabrese, J.R., Gao, K., Miskowiak, K.W., Grande, I., 2018. Bipolar disorders. Nature Reviews Disease Primers 4, 18008.
Wang, J., Wang, Y., Huang, H., Jia, Y., Zheng, S., Zhong, S., Chen, G., Huang, L., Huang, R., 2020a. Abnormal dynamic functional network connectivity in unmedicated bipolar and major depressive disorders based on the triple-network model. Psychological medicine 50, 465–474.
Wang, Y., Gao, Y., Tang, S., Lu, L., Zhang, L., Bu, X., Li, H., Hu, X., Hu, X., Jiang, P., 2020b. Large-scale network dysfunction in the acute state compared to the remitted state of bipolar disorder: A meta-analysis of resting-state functional connectivity. EBioMedicine 54, 102742.
Wang, Y., Wang, J., Jia, Y., Zhong, S., Zhong, M., Sun, Y., Niu, M., Zhao, L., Pan, J., Huang, L., 2017. Topologically convergent and divergent functional connectivity patterns in unmedicated unipolar depression and bipolar disorder. Translational Psychiatry 7, e1165.

Yan, C.-G., Wang, X.-D., Zuo, X.-N., Zang, Y.-F., 2016. DPABI: data processing & analysis for (resting-state) brain imaging. Neuroinformatics 14, 339–351.
Yang, S., 2014. A comparison of different methods of zero-inflated data analysis and its application in health surveys 16, 518–543.
Young, R.C., Biggs, J.T., Ziegler, V.E., Meyer, D.A., 1978. A rating scale for mania: reliability, validity and sensitivity. The British journal of psychiatry 133, 429–435.
Yuan, Y., Zhang, L., Li, L., Huang, G., Anter, A., Liang, Z., Zhang, Z., 2019. Distinct dynamic functional connectivity patterns of pain and touch thresholds: A resting-state fMRI study. Behavioural Brain Research 375, 112142.
Yurgelun-Todd, D.A., Gruber, S.A., Kanayama, G., Killgore, W.D., Baird, A.A., Young, A. D., 2000. fMRI during affect discrimination in bipolar affective disorder. Bipolar disorders 2, 237–248.
Yusuf, O., Bello, T., Gureje, O., 2017. Zero inflated poisson and zero inflated negative binomial models with application to number of falls in the elderly. Biostatistics and Biometrics Open Access Journal 1, 69–75.